THE INSTITUTE OF ELECTRONICS,
INFORMATION AND COMMUNICATION ENGINEERS

IEICE Technical Report
PEM2015 FA-2 (2015-11)

Validated Reactive EM Near-field Phasor Measurement System Using Active Optical Sensors

Sven Kuehn † Serge Pfeifer ‡ Eugene Grobbelaar ‡ Peter Sepan ‡ Beyhan Kochali ‡ and Niels Kuster †

† IT'IS Foundation, ETH Zentrum, ETZ, Zurich, Switzerland

‡ Schmid & Partner Engineering AG, Zurich, Switzerland

E-mail: † kuehn@itis.ethz.ch

Abstract Correlation of close near-field measurements with radiated field patterns will mitigate test efforts for electromagnetic compatibility (EMC) testing and antenna characterization. A novel automated reactive near-field testbed based on photonic phasor probes is presented. The scanning system combines a large scanning volume with micrometer resolution. An optical surface reconstruction system allows the structure of the device under test (DUT) to be measured with better than 20 µm uncertainty, allowing scans at a precisely known distance above arbitrary electronic components. Miniaturized active microphotonic electric and magnetic field probes for the 0.01 – 6 GHz frequency range, combined with a high-speed vector signal analyzer, are applied to measure the electromagnetic (EM) phasor-field distribution with a dynamic range of >120 dB. The fully isolated probes eliminate perturbations of the EM fields generated by the DUT compared to electrically connected near-field probes and offer up to 60 dB better sensitivity than passive electro-optical probes. The testbed allows high-precision broadband near-field 3D scans for antenna characterisation to be performed with excellent inter-laboratory repeatability. The phasor measurement capability enables near- to-far-field transformation and thus direct correlation of near- field and radiated characteristics.

Keywords reactive near field, photonic sensors, phasor, radiation pattern, measurement

1. Introduction

Wireless device manufacturers work under constant competitive pressure to miniaturize and streamline their products while simultaneously adding and enhancing functionality and shortening time-to-market. The trend towards increased miniaturization requires the electronic components to be placed closely together. Space for antennas is limited, and mutual influence with other parts can impair the antenna performance. Today, over-the-air performance of antennas is typically measured in the far-field of the device under test (DUT). The lack of correlation between far-field performance and the actual near-field properties of individual components can result in the need to perform time-consuming trial-and-error processes during antenna optimization. A dual near-field and radiated characteristics testbed that uses the same near-field scans is the ideal solution to address the aforementioned test issues. Far-field radiated fields can be calculated form near-field measurements by various techniques [1]–[6]. The application of these techniques, however, requires precise knowledge of the complex-valued EM near-field (amplitude and phase) and spatial location. An ideal near-field measurement tool should deliver full spectral amplitude and phase information over a large bandwidth, with minimal impact on the measured field and with fine spatial resolution.

2. Objectives

The aim of the presented work was the development of active microphotonic sensors for EM near-field phasor measurements in the radiofrequency (RF) domain. For use of the probes for reactive near-field antenna analysis with far- field transformation and correlation capability, the goal was also to integrate the sensors into a fully automated µm-resolution near-field testbed and thus establish the first near- field scanning system that enables absolute and traceable EM field phasor measurements.

3. Methods

3.1 Microphotonic Phasor EM Near-field Probes

The near-field probe systems applied in the scanner use direct laser modulation for signal transmission and electrically small transducers to pick up the electric (E) or magnetic (H) fields. The system consists of a sensor head and a remote unit (Fig.1), as described in [7]. Each probe contains a sensor head and a sensor identifier (ID). The sensor head is located at the very tip of the probe and contains the actual miniaturized electric or magnetic field sensors, while the sensor ID is located in the rear of the probe body. The sensor ID uniquely identifies each probe to

the remote unit and provides a redundant optical link, which is continuously monitored for LASER safety. The remote unit acts as the photonic power supply in the power-over-fiber forward link. At the sensor head, the photonic energy is converted into electrical energy from which the active elements in the sensor head are supplied. The sensor head uses electrically small transducers to pick up the EM fields. The RF signal from the transducer is amplified by a low noise amplifier (LNA) and modulates the photonic output of a high-speed vertical cavity surface emitting LASER (VCSEL). The signal from the VCSEL is then transmitted to the remote unit via fiber optics. At the remote unit, the photonic signal is demodulated by means of a high-speed photodiode (PD), amplified by a transimpedance amplifier (TIA), and made available over a standard 50Ω output to connect the vector signal analyser in the developed scanning system. This sensor concept allows highly sensitive, fully electrically isolated miniature near-field sensors with a large bandwidth of 10 MHz – >6 GHz to be designed. Due to its large bandwidth and optimized flat frequency domain response, i.e., that presents a non-dispersive system for wide- band signals, we call our sensor implementation TDS for time domain sensors. The probes have been adapted for use inside the scanning system to support automatic probe exchange and more than 25,000 mating cycles of the fiber optic connectors (Fig. 2).

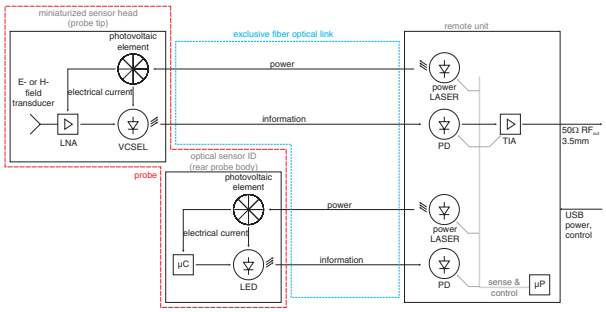

Fig. 1 Schematic diagram of the active electro-optical sensor platform, consisting of a miniature sensor head that is exclusively linked via fiber optics to a remote unit.

Fig. 2 TDS probes for the measurement of electric (blue) and magnetic (red) RF fields optimized for near-field scanning usage. Shown on the left are the probes located in the probe repository inside the developed near-field scanning system. A single E-field probe with a detailed view of the fiber optic machine adapter that allows up to 25,000 probe matings is shown on the right.

3.2 Near-field Phasor Testbed

Fig.3 shows a schematic diagram of the developed near- field testbed with the integrated TDS probes. It is a complete near-field testbed, composed of a shielded anechoic chamber in which the actual near-field scans are performed, positioned on top of an equipment rack that contains all necessary control and measurement equipment. The positioning system consists of gantry type motion stages that allow precise positioning of the probe and also enable the probe to be turned around its axis. The positioning system contains LASER triangulation and camera systems fixed to the z-axis that allow photographs of the DUT to be taken for reconstruction of the surface profile of the DUT to be performed before the actual scans are initiated. Based on the profile of the DUT, scans conformal to the surfaces of arbitrary electronic components can be performed without the need for CAD data input or problematic mechanical surface detection. In the postprocessing software, the photographs of the DUT can be texture mapped onto the profile, and the measured EM results can be displayed overlaid directly on the DUT image.

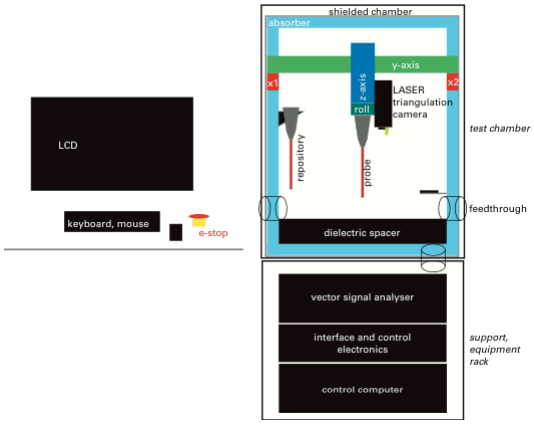

Fig. 3 Schematic diagram of the active electro-optical sensor platform, consisting of a miniature sensor head exclusively linked via fiber optics to a remote unit.

3.3. Validation Sources

Fig. 4(a) shows the validation source for reactive near-field phasor measurements based on a simple μstripline design. For the purpose of the experimental validation, the phasor distribution of the EM structure was simulated numerically with SEMCAD X (SPEAG, Switzerland). Fig. 4(b) shows the validation source for the near-to-far-field transformation that is based on a dipole resonant at 835 MHz. For the purpose of the experimental validation, the near-field phasor distribution and radiation pattern of the dipole were simulated numerically.

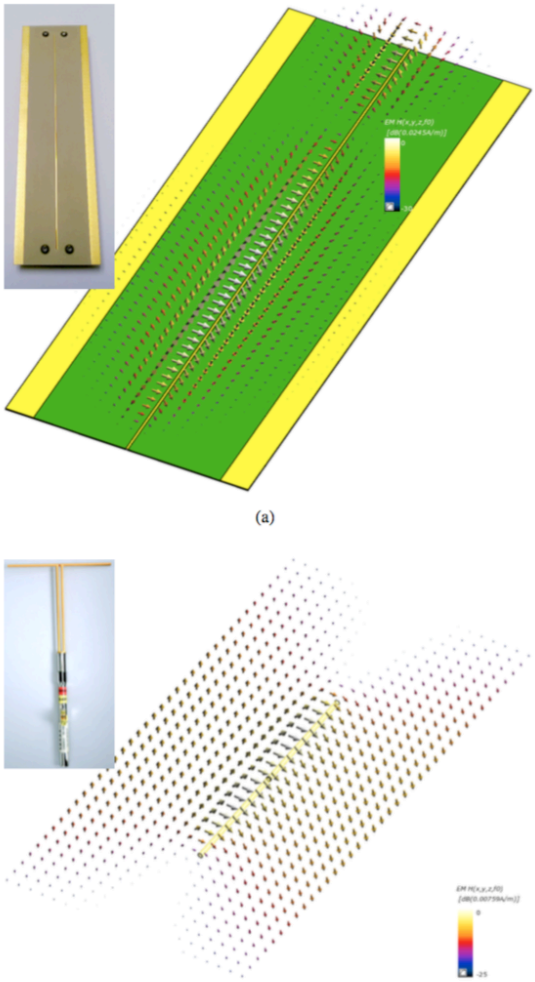

Fig. 4 Near-field and far-field validation sources. Numerical and experimental models of the near-field phasor validation source based on ustripline structure (a) and 835MHz dipole used as validation source for the near-to-far-field transformation (b).

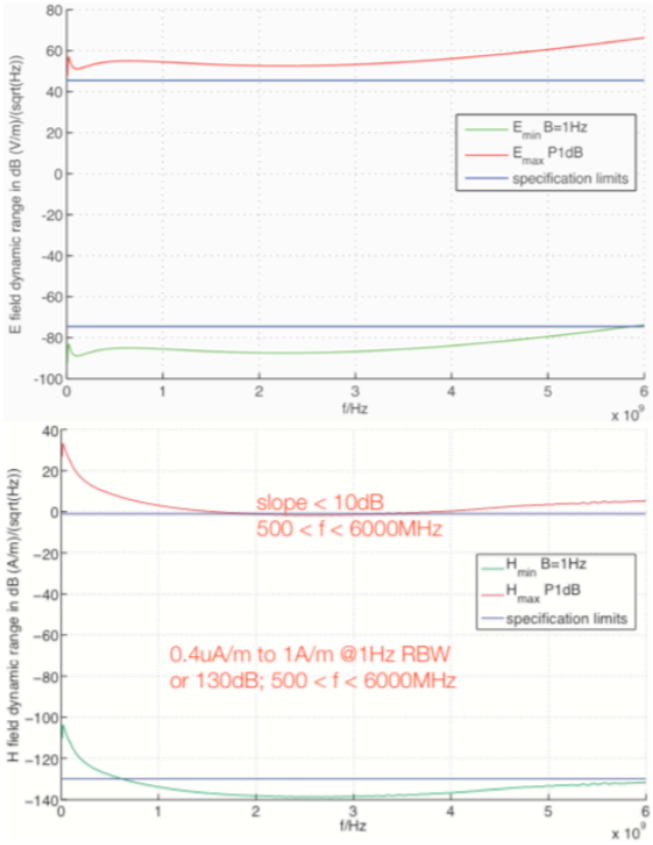

Fig. 5 Dynamic range upper (1dB compression point) and lower (displayed average noise floor) detection limits over the frequency of E1TDS (top) and H1TDS (bottom) probes. Dynamic range upper limit curve is inversely proportional to the probe sensitivity.

4. Results

4.1 Phasor Probe Characteristics

We have developed four types of 1D E- and H-field sensors — based on the active microphotonic sensor platform — that cover orthogonal vector components and are capable of measuring the full EM phasor in the scanning system. The H1TDS and E1TDS sensors were characterized in a waveguide-based calibration system [8] in the frequency range from 0.01 – 6 GHz. Fig. 5 shows the frequency response of the E1TDS and H1TDS probe systems. Both probe types show a very flat frequency response over a large bandwidth and dynamic range. This feature allows the probes to be applied for both frequency domain measurements and wideband time domain measurements without requiring dispersion corrections due to a varying frequency domain response.

4.2 Near-field Scanner

Fig. 6 shows the developed near-field testbed consisting of a shielded testbed chamber with a positioner system. Ferritebacked flat RF absorbers that reduce the reflections from the sidewalls of the shielded chamber surround the measurement volume. A dielectric spacer of laminated glass is placed on top of the bottom absorber to form a stable measurement platform. When the DUT is placed on the glass platform, the system simulates approximately free-space conditions. Alternatively, a ground plane panel can be inserted on top of the platform, to introduce an additional electrically conductive boundary condition at the bottom (e.g., simulating a metallic housing below the DUT). The camera and LASER triangulation systems are attached on the z-axis of the positioner system to provide functionality for scanning the entire measurement volume. The camera has a resolution of 0.07 × 0.07 mm2/pixel. As the camera can be moved, a coarse pre-detection of the DUT elevation profile can be performed based on stereovision and synthetic aperture principles. The fine detection of the DUT's

geometrical structure is based on the LASER triangulation sys- tem, with the algorithms for sub-pixel LASER-line detection [9] and adaptive reflection removal implemented in our system reaching a resolution of better than 20µm. On the left side of the testbed chamber, a probe repository that holds up to four different probes is installed. The positioner system can exchange the probes automatically. This feature allows fully automated scans to be performed, even if multiple probe types are required for full phasor measurements. This is particularly useful for measurements whereby millions of measurement points must be acquired, which requires measurement times easily spanning several hours. The control software of the scanner was designed to maximize autonomous operation. User interaction is required only at the beginning of the scanning process and not for the full duration of the time- consuming scans.

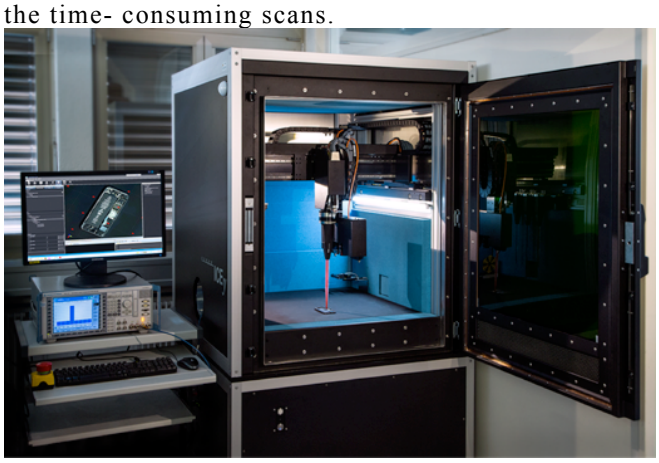

Fig. 6 Photograph of the antenna near-field testbed prototype. Shown is the shielded testbed containing the x,y,z, roll positioners, the probe repository, and the camera and LASER triangulation modules. The testbed is positioned on top of the equipment rack. The operator station is located to the left of the testbed.

4.3 System Validation

The microstripline structure was used to validate the performance of the near-field testbed by mapping the reactive near-field H-field phasor on top. The measurement results compared to the numerical targets are displayed in Figs. 7,8. A full EM phasor near-field scan on a closed surface (in this example, because of symmetry, measured on one half- surface and mirrored) around the 835MHz validation dipole was performed to validate the near-to-far-field transformation capability of the system.

The near-field results illustrate the measurement accuracy of our TDS probes and scanning system. Despite a strong field gradient in the near-field of the source, our miniature field probes can accurately resolve the magnetic phasor field distribution. With the completely isolated sensor design, adverse loading of the source is prevented even at very close distances.

The extrapolated far-field radiation pattern results (Fig. 10) demonstrate the system's capability to perform analyses of the radiated characteristics based on reactive near-field scan results. It is demonstrated that the Eθ component of the dipole validation source can be accurately reconstructed in the far- field.

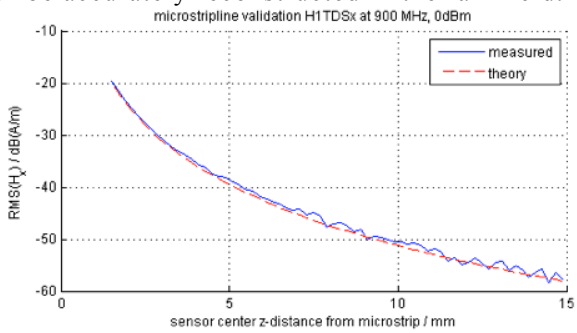

Fig. 7 H-field (magnitude) validation measurement result of the radial component on top (over distance) of the microstripline validation structure measured with an H1TDSx probe and comparison to the analytical target.

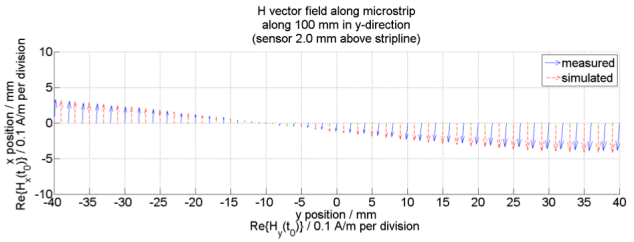

Fig. 8 Validation measurement result of the phasor field on top of the microstripline validation structure measured with H1TDSx probe and comparison to the simulated target with SEMCAD X (SPEAG, Switzerland).

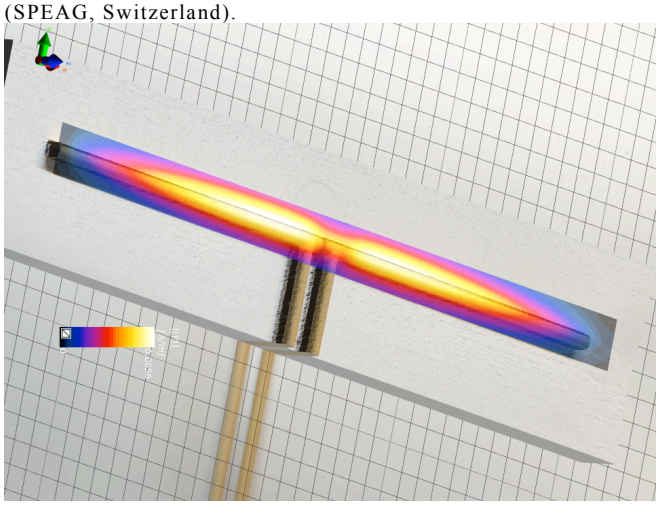

Fig. 9 Reactive near-field scan result around the 835MHz dipole.

5. Conclusions

We have developed an automated near-field testbed for reactive near-field EM phasor characterisation in the RF domain with the capability to perform near-to-far-field transformations for the analysis of radiated characteristics based on the same scans. The scanning system combines a large scanning volume of 500 × 500 × 100 mm3 with micrometer resolution.

A novel optical surface reconstruction system allows the surface profile of the DUT to be measured with better than 20 µm uncertainty. This allows for scanning at a precise distance above arbitrary electronic components. Active micro-photonic ultra-wideband E- and H-field sensors for the frequency range from 0.01 – 6GHz combined with a high-speed vector signal analyser are applied to measure the EM phasor with a dynamic range of >120 dB. Compared to electrically connected probes, our microphotonic probes eliminate the disturbance of the fields of the DUT as they are fully electrically isolated and offer up to 60dB better sensitivity than passive electro-optical probes, making them a tool of choice for this application. The applicability of our measurement system to reactive near-field EM phasor scanning tasks and near-to-far-field transformations has been successfully demonstrated. The system allows high- precision broadband near-field 3D scans for EMC/EMI and antenna analysis to be performed with excellent inter-laboratory repeatability.

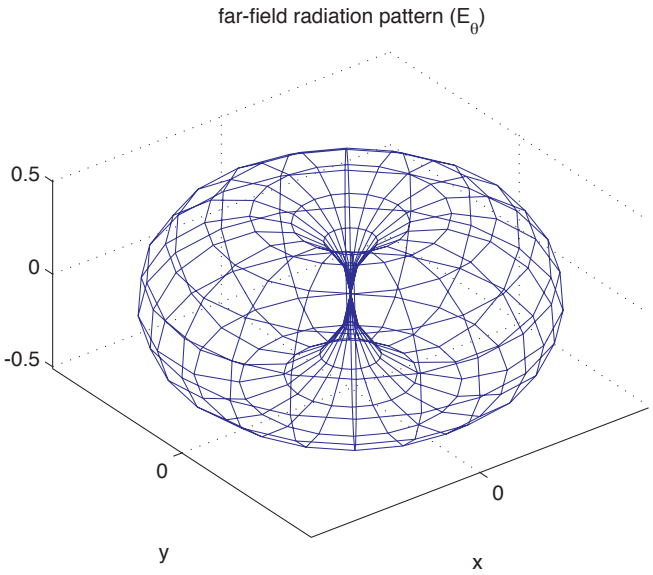

(a) Far-field radiation pattern of the Eθ component

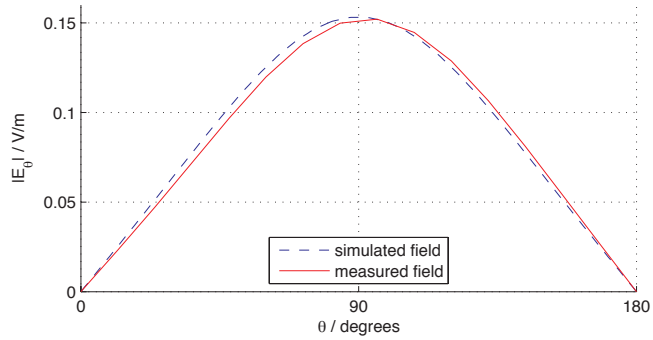

(b) Comparison of the measured far-field radiation pattern Eθ component (red) with the numerical target (blue) (both based on near-to-far-field trans- formation)

Fig. 10 Far-field extrapolation result based on reactive near-field phasor measurements around a 835 MHz dipole.

References

[1] A. Taflove, S. C. Hagness *et al.*, "Computational electrodynamics: the finite-difference time-domain method," *Norwood, 2nd Edition, MA: Artech House, l995*, 1995

[2] P. Petre and T. K. Sarkar, "Differences between modal expansion and in- tergral equation methods for planar near-field to far-field transformation," *Progress In Electromagnetics Research*, vol. 12, pp. 37–56, 1996.

[3] X. Gao, J. Fan, Y. Zhang, H. Kajbaf, and D. Pommerenke, "Far- field prediction using only magnetic near-field scanning for emi test," Electromagnetic Compatibility, IEEE Transactions on, vol. 56, no. 6, pp. 1335–1343, 2014.

[4] C. H. Schmidt, M. M. Leibfritz, and T. F. Eibert, "Fully probe-corrected near-field far-field transformation employing plane wave expansion and diagonal translation operators," Antennas and Propagation, IEEE Trans- actions on, vol. 56, no. 3, pp. 737–746, 2008.

[5] C.-C. Oetting and L. Klinkenbusch, "Near-to-far-field transformation by a time-domain spherical-multipole analysis," Antennas and Propagation, IEEE Transactions on, vol. 53, no. 6, pp. 2054–2063, 2005.

[6] H. Weng, D. G. Beetner, and R. E. DuBroff, "Prediction of radiated emissions using near-field measurements," Electromagnetic Compatibility, IEEE Transactions on, vol. 53, no. 4, pp. 891–899, 2011

[7] A. Kramer, P. Mu¨ller, U. Lott, N. Kuster, and F. Bomholt, "Electro- optic fiber sensor for amplitude and phase detection of radio frequency electromagnetic fields," Optics letters, vol. 31, no. 16, pp. 2402–2404, 2006.

[8] .Pokovic,"Advancedelectromagneticprobesfornear-f ieldevaluations," Ph.D. dissertation, Diss. Techn. Wiss. ETH Zu¨rich, Nr. 13334 1999. Ref.: N. Kuster; Korref.: H. Baltes; Korref.: Q. Balzano, 1999.

[9] J. Forest Collado et al., New methods for triangulation-based shape acquisition using laser scanners. Universitat de Girona, 2004.